32ND INTERNATIONAL COSMIC RAY CONFERENCE, BEIJING 2011


# Observation of Anisotropy in the Arrival Direction Distribution of Cosmic Rays at TeV Energies with IceCube

THE ICECUBE COLLABORATION[1]
[1]*See special section in these proceedings*

**Abstract:** The IceCube neutrino detector at the South Pole is sensitive to atmospheric muons produced by primary cosmic rays in the TeV energy range. The high rate of events (about 2 kHz in the full 86-string detector) allows for searches of anisotropy in the arrival direction distribution of cosmic rays at the level of a few parts per mille. Using the muon data recorded with IceCube between 2007 and 2010, we show that the cosmic ray flux in the southern hemisphere is not isotropic, but exhibits significant structure on multiple angular scales. In addition to large-scale features in the form of strong dipole and quadrupole moments, the data include several localized regions of excess and deficit on scales between $10^\circ$ and $30^\circ$. These features are statistically significant. The origin of the features is currently unknown.

**Corresponding Authors:** Segev BenZvi[2] (*sybenzvi@icecube.wisc.edu*), Marcos Santander[2] (*santander@icecube.wisc.edu*), Simona Toscano[2] (*toscano@icecube.wisc.edu*), Stefan Westerhoff[2] (*swesterhoff@icecube.wisc.edu*)
[2]*Dept. of Physics, University of Wisconsin-Madison, Madison, WI 53703, USA*

**Keywords:** Cosmic Rays – TeV; Anisotropy; Muons; Neutrinos

## 1 Introduction

The IceCube detector, deployed between 1450 m to 2450 m below the surface of the South Polar ice sheet, is designed to detect upward-going neutrinos from astrophysical sources. However, it is also sensitive to downward-going muons from cosmic-ray air showers. To penetrate the ice and trigger the detector, the muons must be produced by cosmic rays with energies of at least several TeV. The arrival direction of a cosmic muon is typically within $0.2^\circ$ of the direction of the primary particle, so the arrival direction distribution of muons is also a map of cosmic ray arrival directions between about 1 and several hundred TeV.

At energies of a few TeV, it is believed that galactic magnetic fields should randomize the arrival directions of charged cosmic rays. However, in recent years an anisotropy in the arrival direction distribution has been reported on both large and small angular scales. The anisotropy is observed in the northern sky between several TeV and several hundred TeV by the Tibet AS$\gamma$ array [1], Super-Kamiokande [2], Milagro [3, 4], ARGO-YBJ [5], and EAS-TOP [6]. In 2010, an analysis of muons recorded by the IceCube detector also revealed a large-scale anisotropy in the southern sky [7]. In these proceedings, we present the results of a search of the southern sky for anisotropy on all angular scales using data recorded between May 2009 and May 2010.

## 2 The IceCube Detector and Data

IceCube is a km$^3$-size neutrino detector frozen into the glacial ice sheet at the geographic South Pole. High-energy charged particles passing through the detector emit Cherenkov radiation, and their tracks are recorded by an array of Digital Optical Modules (DOMs) embedded in the ice. The DOMs are attached to 86 vertical cables, or strings (with 60 DOMs per string), which are used to transmit data to the surface. Construction of IceCube was completed in December 2010. The detector has been operating in various configurations since construction began. Between 2007 and 2008, it was operated with 22 strings deployed (IC22), between 2008 and 2009 with 40 strings (IC40), and between 2009 and 2010 with 59 strings.

Muons are identified using a simple majority trigger, which requires 8 or more DOMs in local coincidence within a $5\ \mu$s window. The trigger rate of downgoing muons is 0.5 kHz in IC22, 1.2 kHz in IC40, and 1.4 kHz in IC59, about a factor of $10^6$ larger than the neutrino rate. The rate is too large to transfer complete waveforms for all events via satellite, so the muon data are reconstructed on-line and compressed using a Data Storage and Transfer (DST) format. Muon tracks are identified using a maximum-likelihood reconstruction, and the event arrival direction and energy estimators are stored in DST files and sent north by satellite. Digitized waveforms are discarded due to limited bandwidth.

The analysis presented in this paper uses the DST data collected during IC59 operations between May 20, 2009 and May 30, 2010. The data set contains nearly $3.4 \times 10^{10}$ muon events recorded during a live time of 335.5 days. A cut in zenith angle at $65^\circ$ removes less well-reconstructed tracks near the horizon, reducing the final analysis sample to $3.2 \times 10^{10}$ events. The median angular resolution of events in the sample is $3^\circ$; unlike the neutrino analysis, the cuts have not been optimized for point source identification. Using simulated data, we estimate the median energy of the events to be 20 TeV. The energy resolution of the cosmic ray primaries is about $\Delta \log (E/\mathrm{eV}) = 0.5$.

## 3 Analysis

### 3.1 Calculation of the Reference Level

The arrival direction distribution of cosmic rays in IceCube exhibits anisotropy caused by non-physical effects such as gaps in the detector uptime. These effects must be removed before any physical anisotropy can be identified. Therefore, the first step in the analysis is the creation of a "reference map," a sky map that describes what the arrival direction distribution would be if the cosmic ray flux were isotropic. The reference map must be subtracted from the arrival direction distribution in the data to find regions where the cosmic ray flux deviates from the isotropic expectation.

We estimate a reference map for IC59 data using the time-scrambling method of Alexandreas et al. [8]. The sky is binned into an equal-area grid in equatorial coordinates with $0.9^\circ$ resolution using the publicly-available HEALPix library [9]. From this sample two sky maps are produced. The data map $N(\alpha, \delta)$ stores the arrival directions of all events. For each detected event in the data map, "fake" events are generated by keeping the local zenith and azimuth angles $(\theta, \phi)$ fixed but reassigning the time to that of another event recorded within a pre-defined time window $\Delta t$. The event times within the window are resampled 20 times and used to generate 20 fake celestial coordinate pairs $(\alpha, \delta)$ which are used to fill a reference sky map $\langle N(\alpha, \delta) \rangle$ with a weight of 1/20.

A known disadvantage of the method is that it can be biased by a strong anisotropy, leading to artificial deficits or excesses next to regions of true excess or deficit [3]. However, the procedure does preserve the local arrival direction distribution of the data and naturally compensates for variations in the event rate which are difficult to model, such as changes in atmospheric conditions which affect the production of muons in air showers. The only critical requirement for time scrambling is to choose the buffer length $\Delta t$ such that detector conditions remain stable during this period. Using $\chi^2$ tests to compare the distribution of arrival directions in local coordinates across measurement periods, we have verified that the IceCube detector is stable over periods of at least one full day. In this analysis we choose $\Delta t = 24$ hr.

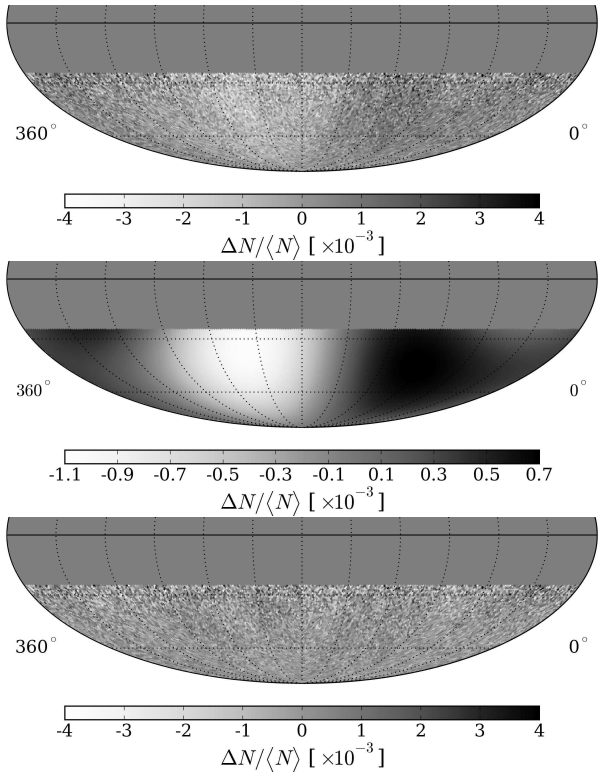


Figure 1: *Top*: Relative intensity of the IC59 data produced with $\Delta t = 24$ hr. *Middle*: Fit of dipole and quadrupole moments to the relative intensity. *Bottom*: Residual map after removal of the dipole and quadrupole.

### 3.2 Relative Intensity

Once the data and reference maps are calculated, deviations from isotropy can be analyzed by computing the relative intensity

$$\frac{\Delta N_i}{\langle N \rangle_i} = \frac{N_i(\alpha, \delta) - \langle N_i(\alpha, \delta) \rangle}{\langle N_i(\alpha, \delta) \rangle}. \quad (1)$$

which gives the amplitude of deviations from the isotropic expectation in each angular bin $i$. The significance of the deviation in bin $i$ can be calculated using the method of Li and Ma [10].

A map of relative intensity of the IC59 data, binned with $0.9^\circ$ resolution, is shown at the top of Fig. 1. The map exhibits obvious correlations between bins, such as a broad excess in the relative counts near $\alpha = 105^\circ$ and a broad deficit near $\alpha = 225^\circ$. The relative intensity in these regions is of order $10^{-3}$. This structure is the large-scale anisotropy reported in the IC22 data by Abbasi et al. [7]. Since the IC59 data set is larger than that of IC22 by an order of magnitude, it is possible to see the large-scale structure in the data without further rebinning.

### 3.3 Removal of Large-Scale Structure

The relative intensity shown at the top of Fig. 1 is dominated by large-scale structures, but there are additional

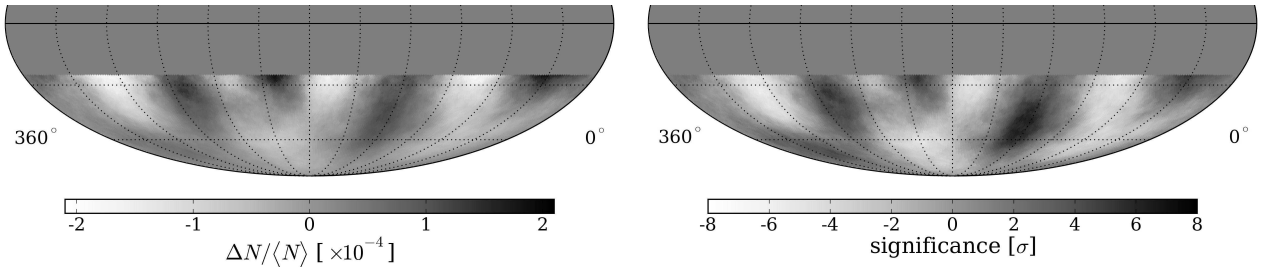


Figure 2: IC59 residual maps after subtraction of dipole and quadrupole moments, showing relative intensity (left) and significance before trial factors are applied (right). The maps have been smoothed with a circular window of $20°$.

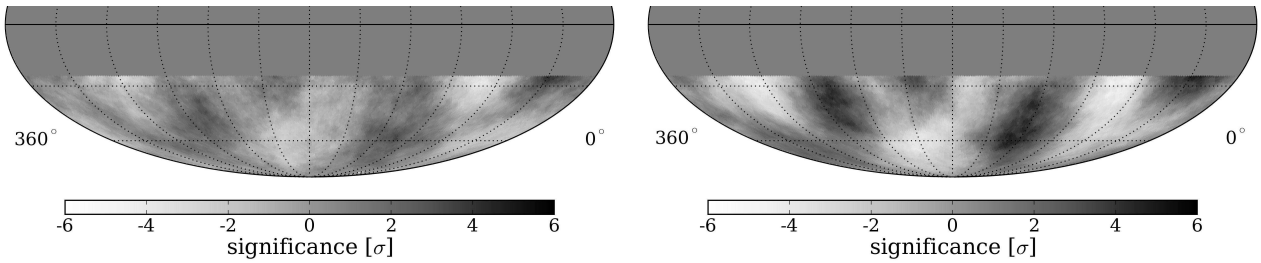


Figure 3: Residual maps from IC22 (left) and IC40 (right) showing the significance of deficit and excess regions with $20°$ smoothing.

small-scale features in the map. This can be demonstrated by calculating the angular power spectrum of the data, which exhibits significant power not only at the largest angular scales, but also down to scales of about $10°$ (see detailed discussion in Abbasi et al. [11]).

We can also demonstrate the presence of small-scale structure by explicitly removing the largest angular correlations in the data. This is accomplished by fitting dipole and quadrupole terms to the relative intensity map and then subtracting the fit to obtain a map of residual counts. In the middle panel of Fig. 1, we show the result of the fit of dipole and quadrupole moments to the intensity map. By themselves, these two terms account for much of the amplitude of the per-mille anisotropy observed in the data. However, the fit $\chi^2/\text{ndf} = 14743/14187$ corresponds to a $\chi^2$-probability of approximately $0.05\%$, suggesting that the dipole and quadrupole are not sufficient to explain all of the structures observed in the angular distribution of $\Delta N/\langle N\rangle$.

Subtraction of the dipole and quadrupole fit from the data gives the bottom panel in Fig. 1. The fit residuals are relatively featureless at first glance, but the bin size is not optimized for a study of significant anisotropy at angular scales larger than the angular resolution of the detector. To increase the sensitivity to the small-scale structure in the data, we apply a smoothing procedure which takes the reference level and residual data counts in each bin and adds the counts from pixels within some angular radius of the bin. This procedure results in a map with Poisson uncertainties, though the bins are no longer statistically independent.

Smoothed residual maps of relative intensity and significance are shown in Fig. 2. To make this figure, a smoothing radius of $20°$ was chosen. Strong regions of excess and deficit are visible in the data. Note that the actual size of any given excess or deficit region (and thus the optimal smoothing scale) is not known *a priori*. Therefore, we study the sky map on all smoothing scales from $3°$ (the angular resolution of the data) to $45°$ in steps of $1°$ and search for regions of high significance at any location.

Applying this procedure, the two most significant features on the sky are a region with a peak significance of $5.3\sigma$ at a smoothing radius of $22°$ ($\alpha = 122.4°, \delta = -47.4°$) and a region of peak significance $4.9\sigma$ at a smoothing radius of $13°$ ($\alpha = 263.0°, -44.1°$). The significance values account for statistical trials due to the scan over smoothing radii and the location of the most significant pixels. The trial factors were estimated using a Monte Carlo simulation of an isotropic flux recorded by the IceCube detector.

## 4 Systematic Checks

Several tests have been performed on the data to ensure the stability of the observed anisotropy and to rule out possible sources of systematic bias. Among the influences that might cause spurious non-physical anisotropies are the detector geometry, the detector livetime, non-uniform exposure of the detector to different regions of the sky, and diurnal and seasonal variations in atmospheric conditions. Due to its unique location at the South Pole, many of these effects play a lesser role for IceCube than for detectors at the middle latitudes. We check the validity of this assumption by searching the data for a signal expected in solar coordinates, and by examining the data from previous configurations of the detector.

### 4.1 Solar Dipole Analysis

The cosmic rays at TeV energies do not co-rotate with the Earth about the Sun, and so it is expected that the flux of cosmic rays should exhibit a dipole modulation in solar coordinates. The expected change in relative intensity is given by

$$\frac{\Delta I}{I} = (\gamma + 2)\frac{v}{c}\cos\theta, \qquad (2)$$

where $I$ is the cosmic ray intensity, $\gamma = 2.7$ is the power law index of the energy spectrum at several TeV, $v/c$ is the ratio of the orbital velocity of the Earth with respect to the speed of light, and $\theta$ is the angle between the cosmic ray arrival direction and the direction of motion of the Earth. Given $v = 30$ km s$^{-1}$, we expect an amplitude of $4.7 \times 10^{-4}$.

The solar dipole provides a convenient measurement with which to check the analysis technique. The reference and data maps were computed in solar coordinates, and the relative intensity map has been fit with a dipole function. A single dipole describes the data quite well: the fit $\chi^2/\text{ndf} = 14206.8/14192$ corresponds to a $\chi^2$-probability of 41.6%. The dipole is aligned at a longitude of $270^\circ$ in solar coordinates, following the expectation for a relative-motion anisotropy in this coordinate frame. Its amplitude is $(3.66 \pm 0.14 \pm 0.99) \times 10^{-4}$, in agreement with the expectation within the large systematic uncertainty. A more detailed study of the solar dipole anisotropy is presented in Abbasi and Desiati [12].

### 4.2 Anti-Sidereal Time Analysis

Seasonal variations in the solar dipole anisotropy can create spurious signals in equatorial coordinates, and vice-versa. We study this effect using an artificial time scale called anti-sidereal time, which is calculated by reversing the sign of the transformation between universal time and sidereal time. No physical anisotropy is expected in this reference frame, but it can be used to identify systematic distortions due to seasonal effects.

We have produced sky maps using anti-sidereal coordinates and performed the same analysis presented in Section 3. No regions of significant excess or deficit are observed in the anti-sidereal maps for any smoothing scale. A detailed discussion is provided in [11].

### 4.3 Comparison to IC22 and IC40 Data

An important cross-check of the IC59 analysis can be made by applying the same method to data recorded in the two data periods prior to IC59. The IC22 data set contains $4 \times 10^9$ events recorded between July 2007 and April 2008, and the IC40 data set contains $1.9 \times 10^{10}$ events recorded between April 2008 and April 2009. While the samples are smaller than IC59, we expect to observe the most prominent structures in these data, albeit with reduced significance. The IC22 and IC40 data can be used to verify that the structures observed in the arrival direction distribution do not depend on the geometry of the detector or the data-taking period. For example, the shape of IC22 was highly asymmetrical, with a long and a short axis.

In Fig. 3, we show the residual maps from IC22 and IC40 after the subtraction of dipole and quadrupole terms and smoothing by $20^\circ$. While none of the features in IC22 and IC40 have a pre-trial significance above $5\sigma$, they align with the regions of deficit and excess observed with IC59 data (cf. Fig 2). The main features on both large and small scales appear to be persistent in all data sets.

## 5 Conclusions

Using $3.2 \times 10^{10}$ events recorded with the partially-deployed IceCube detector between May 2009 and May 2010, we have found that the arrival direction distribution of cosmic rays at several TeV exhibits significant anisotropy on several angular scales. The data are dominated by dipole and quadrupole moments, but there is also significant structure on angular scales down to about $10^\circ$. These structures become visible in the sky map when the dominant terms are subtracted.

There is currently no explanation for these local enhancements in the cosmic ray flux, and so the study of cosmic ray arrival directions in the TeV region will continue to be a major ongoing effort in IceCube. We are currently studying the anisotropy in the 79-string configuration of the detector (IC79). During the next several years, with the IceCube detector operating in its complete 86-string configuration, the data will increase by $4.5 \times 10^{10}$ events per year. With these high statistics we will be able to study possible time dependencies in the anisotropy and compare to similar studies in the northern hemisphere [4, 13]

## References


[1] M. Amenomori et al., Astrophys. J., 2005, **626**: L29
[2] G. Guillian et al., Phys. Rev., 2007, **D75**: 062003
[3] A.A. Abdo et al. Phys. Rev. Lett., 2008, **101**: 221101
[4] A.A. Abdo et al. Astrophys. J., 2009, **698**: 2121
[5] S. Vernetto et al. Proc. 31st ICRC, 2009, Łódź, Poland
[6] M. Aglietta et al. Astrophys. J., 2009, **692**: L130
[7] R. Abbasi et al., Astrophys. J., 2010, **718**: L194
[8] D.E. Alexandreas et al., NIM A, 1993, **328**: 570
[9] K.M. Gorski et al., Astrophys. J., 2005, **622**: 759
[10] T.-P. Li and Y.-Q. Ma, Astrophys. J., (1983), **272**: 317
[11] R. Abbasi et al., arXiv:1105.2326 [astro-ph], submitted to Astrophys. J., 2011
[12] R. Abbasi and P. Desiati, these proceedings.
[13] M. Amenomori et al., Astrophys. J., 2010, **711**: 119